Article

Lake Expansion under the Groundwater Contribution in Qaidam Basin, China

Xi Zhang [1], Jiaqi Chen [2,*], Jiansheng Chen [3], Fenyan Ma [3] and Tao Wang [4]

[1] School of Earth Sciences and Engineering, Hohai University, Nanjing 211100, China; zhangxi19@hhu.edu.cn
[2] College of Computer and Information, Hohai University, Nanjing 211100, China
[3] College of Civil and Transportation Engineering, Hohai University, Nanjing 210098, China; jschen@hhu.edu.cn (J.C.); fyma@hhu.edu.cn (F.M.)
[4] College of Water Conservancy and Hydropower Engineering, Hohai University, Nanjing 210098, China; wangtao77@hhu.edu.cn
[*] Correspondence: jiaqichen@hhu.edu.cn

Abstract: The relationship between groundwater and lakes in Qaidam Basin is often overlooked. Therefore, we employed Landsat satellite images and meteorological data to investigate the causes of lake expansion through model calculation and statistical analysis and then determine groundwater sources through isotope analysis (^{2}H, ^{3}H, and ^{18}O). In the two study periods of 2003–2011 and 2011–present, temperature, precipitation, and runoff increased at a steady rate, whereas the expansion rate of Tuosu Lake increased from 1.22 km^2/year to 3.38 km^2/year. This significant increase in the rate of lake expansion reflects the substantial contribution of groundwater to lake expansion. The groundwater contribution to the lake includes not only the glacial meltwater that infiltrates the piedmont plain but also other, more isotopically deleted water sources from other basins. It is speculated that the 2003 M$_s$ 6.4 earthquake in the northwest of the Delingha region was a possible mechanism for lake expansion. Earthquakes can enhance crustal permeability and keep fractures open, which promotes groundwater contribution to lakes and in turn causes rapid lake expansion and an increased groundwater level. This study is important for understanding the sources, circulation, and evolution of groundwater in Qaidam Basin.

Keywords: Qaidam Basin; lake expansion; groundwater contribution; oxygen and hydrogen isotopes; climate change

1. Introduction

In recent decades, many lakes in the Tibetan Plateau have exhibited continued and rapid expansion [1–3], in contrast to a general trend of lake shrinkage in other regions and basins around the world. Qaidam Basin, located in the northeastern margin of the Tibetan Plateau, is an arid alpine region with scarce precipitation and intense evaporation. Thus, the regional hydrological cycle is sensitive to both climate change and human activity. As an important part of the hydrological cycle in arid areas, lakes are possibly affected by climate change processes such as increased precipitation and temperature [3,4]. For example, higher temperatures accelerate glacier melting and increase runoff into the lake, leading to lake expansion. Simultaneously, increased precipitation may partly contribute to lake expansion [5–7].

In addition to climate change, the impact of groundwater contribution to lakes should also be considered. The role of groundwater in lakes has previously been observed in Qinghai Lake [8] (China), Nalengele River [9] (China), Pyhajarvi Lake (Finland) [10], and other basins [11], although the sources of groundwater have not been thoroughly studied. A recent study [12] revealed that the endorheic Qiangtang Basin has a large amount of missing water (up to 540×10^8 m^3/year), which leaks through six rifts in the south of the basin and may subsequently upwell in surrounding areas. This observation invalidates the

traditional water budget theory of watersheds and likely also affects the water budget of surrounding areas. Qaidam Basin, which is adjacent to Qiangtang Basin, is a key area for water discharge. Studies of radon (^{222}Rn) isotopes have revealed that lakes in the Qaidam Basin have an extensive groundwater contribution [9,11]. Therefore, in this study, we investigated lake surface area changes in response to climate change and groundwater contributions in the northeast of Qaidam Basin, which is important to understand the sources, circulation, and evolution patterns of regional groundwater.

The expansion or shrinkage of a lake directly reflects the lake water budget. In inland basins of alpine regions, mountain precipitation and/or glacial meltwater converge into rivers. When these rivers flow through the piedmont plain, some of the water infiltrates as groundwater, and some continues to flow downstream, flowing through alluvial plains to eventually form endorheic lakes. Endorheic lakes are generally located at the lowest elevation in the basin, where they form a confluence of surface water [9,13]. The regional distribution of groundwater heads determines whether the lake discharges to groundwater or groundwater contributes to the lake, which controls groundwater inflow and outflow in the water balance of the endorheic lake. The groundwater level in Qaidam Basin gradually decreases from the mountains to the plains; thus, groundwater flows from the mountains to the lakes in the plains, where it eventually contributes to the lakes [8,9,11]. Therefore, the water input component of these endorheic lakes predominantly includes surface runoff, lake precipitation, and groundwater inflow, and the water output component is principally lake evaporation; groundwater outflow can typically be ignored [14].

Thus, it is important to accurately quantify lake evaporation before exploring the causes of lake expansion. By comparing the eddy covariance system with several combined evaporation models, McJannet [15,16] concluded that the Penman–Monteith model was most suitable for estimating lake evaporation because it considers the effects of both vapor pressure gradient and wind speed. However, the meteorological monitoring network in alpine areas is typically sparse, with stations often located far from lakes; therefore, it is difficult to obtain long time-series of meteorological monitoring data near lakes. The improved Penman–Monteith model proposed a general application of wind functions and thus can be used to calculate lake evaporation from remote overland meteorological measurements [15,16], which has been applied in several subsequent studies. Lake surface area changes can also reflect changes in lake water storage [17–19]. However, because of the remote environment and lack of monitoring stations, lakes in the Tibetan Plateau lack long-term monitoring data related to water levels and lake surface area. Thus, satellite remote sensing technology is used in this study to observe long-term changes in lake surface area and water level [2,4,20,21]. Moreover, ^{2}H and ^{18}O isotopes in water bodies are ideal natural tracers for identifying groundwater sources and tracing hydrologic cycles [11,13]. Furthermore, tritium (^{3}H) can determine the rate of groundwater circulation and the groundwater age [20].
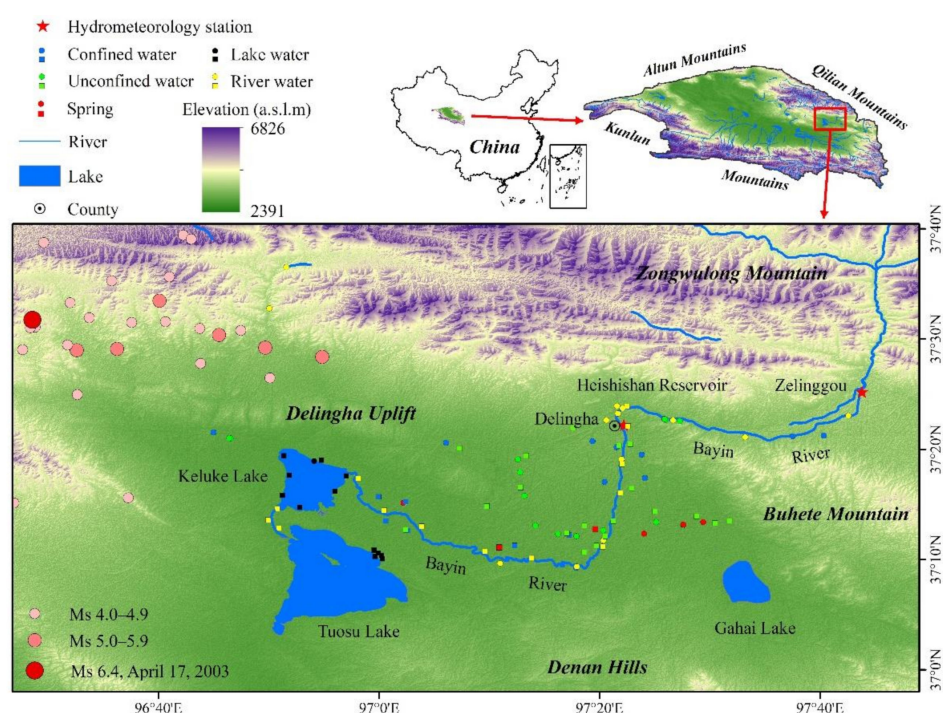
We investigated three lakes in this study (Tuosu Lake, Keluk lake, and Gahai Lake), all of which are located in the northeast of the extremely arid Qaidam Basin. Remote sensing techniques, model calculations, and statistical analyses were used to analyze lake surface area changes in response to climate change and groundwater contribution in the study area, and potential groundwater sources were identified using stable isotopes. The aims of this study were to (1) provide scientific support for the utilization and management of water resources in Qaidam Basin and (2) propose measures for mitigating future environmental and geological problems related to continued lake expansion, thereby protecting inhabitants and production in the study region.

2. Study Region

The study area (96°34′–97°54′E, 36°58′–37°40′N) is located in the northeast of Qaidam Basin, China, which is surrounded by the Buhete Mountains to the east, the Delingha uplift to the west, the Denan hills to the south, and the Zongwulong Mountains to the north (Figure 1). The landscape is predominantly mountainous, alluvial–proluvial plain,

and alluvial lacustrine plain. The study area has a typical plateau continental climate, with annual average temperature, precipitation, and pan-evaporation values of 4.7 °C, 211 mm/year, and up to 1845 mm/year, respectively.

The main river (Bayin River) in the study area originates from the Zongwulong Mountains and has a total length of 188 km and a catchment area of 7281 km^2. The Bayin River flows east to west between Zongwulong and Buhete Mountains and then north to south after flowing through the Heishishan reservoir [11]. The Bayin River seeps underground in the middle of the alluvial–proluvial plain and then upwells as springs at the front edge of the alluvial plain. Because of the influence of the Denan hills, the Bayin River flows westward downstream across the alluvial lacustrine plain and eventually flows into Keluke Lake. Keluke Lake is connected to Tuosu Lake by the Lianshui River, forming a terminal endorheic lake. Gahai Lake is another terminal endorheic lake located in the southeast of the study area, which has a weak hydraulic connection with the Bayin River through southeast groundwater runoff.

Figure 1. Spatial map representing the distribution of samples, including river, lake, spring, confined groundwater, and phreatic groundwater in the northeast of the Qaidam Basin, China. Squares represent samples from the literature [11].

Groundwater in the Delingha area mainly occurs in porous quaternary loose sediments in the plain areas. At the top and middle of the alluvial–proluvial plain, the single-layer alluvial aquifer is more than 300 m thick and mainly composed of sand and gravel; the depth of the groundwater level is 80–120 m and 10–30 m, respectively. At the end of the alluvial–proluvial plain, the aquifer system changes from a single-layer structure to a multi-layer structure, sediments are mostly fine-grained, and the groundwater level is shallow (<10 m) [13]. In the lacustrine plain downstream of Bayin River, the aquifer system consists of a multi-layer aquifer with interbedded clay and fine sand. In the study area, groundwater flows from south to north in the upper part of the alluvial–proluvial plain and then flows westward again because of the effect of the Denan hills [21], which are predominantly tertiary clastic rocks interspersed with mudstone and gypsum with limited infiltration capacity. In addition, the scarce precipitation and low precipitation intensity (a single precipitation event is less than 10 mm) hinders groundwater formation. In the western part of the alluvial–proluvial plain, groundwater flows from north to south and

southeast because of the Delingha uplift, before finally flowing westward [11]. In the eastern part of the alluvial–proluvial plain, a small amount of groundwater flows southeast along the ancient river channel and converges at Gahai Lake.

Since 2000, Tuosu and Gahai Lakes have exhibited rapid expansion. The continuous expansion of Gahai Lake has caused groundwater levels to rise in the vicinity, which threatens the safety of inhabitants and their livelihoods. Therefore, the causes of lake expansion have become a key area of research for local governments. Delingha has a permanent population of 88,200 and a population density of only 2.88 people/km^2 (the seventh National Census). Because of their remote environment and minimal human impact, the lakes in the study area are suitable for studying the effects of climate change and groundwater on lake expansion.
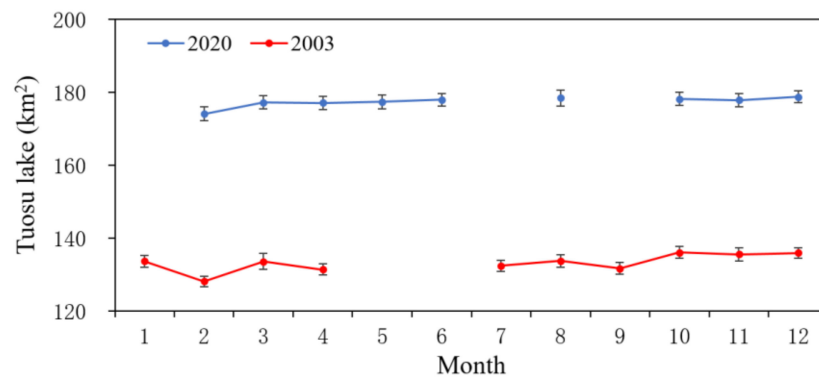
The Bayin River has two hydrologic stations (Figure 1), the Delingha (96°16′E, 37°22′N) and Zelinggou stations (97°48′E, 37°25′N). Zelinggou station is located 7 km upstream of Delingha station, near the exit of the mountain. The runoff measured at this station is mainly glacial meltwater from the mountainous area; hence, Zelinggou station runoff represents the amount of glacier melt in the lakes. The catchment between Delingha and Zelinggou station is defined as the upstream area. The runoff measured at Delingha station includes glacial meltwater and runoff generated by precipitation in the upstream area. The monitoring period for Zelinggou station was 1959–1984, as the station was withdrawn after 1984. Data from these hydrological stations were used for subsequent statistical analysis of runoff trends.

3. Methods

3.1. Landsat Data and Lake Surface Area Extraction

Long-term changes in the surface area of Tuosu, Keluke, and Gahai Lakes were extracted from remote sensing images. Since 1984, Landsat satellites have acquired high-resolution Earth observation images, which are widely used for feature identification. In this study, the Landsat 5 Thematic Mapper (TM) and Landsat 8 Operational Land Imager (OLI), which are the longest time-series data currently available, provided observation data for different periods. The Universal Transverse Mercator (UTM) and World Geodetic System 1984 were used as geocoordinate references to construct the temporal and spatial sequence of lake changes. The spatial resolution of the extracted lake surface area was 30 m, which is sufficient for studying lakes measuring several tens to hundreds of square kilometers. Although the spatial resolution is moderate, its effect on the results is very limited [22–25]. All Landsat data were downloaded from the United States Geological Survey (http://glovis.usgs.gov/, accessed on 10 January 2021), Geospatial Data Cloud (https://geocloud.cgs.gov.cn/, accessed on 10 January 2021), and Chinese Academy of Sciences (http://www.gscloud.cn/, accessed on 10 January 2021). The necessary image pre-processing steps, such as radiation calibration and atmospheric correction, were performed using ENVI 5.3 software.

The repeat coverage of Landsat 5 and Landsat 8 is 18 and 16 days, respectively, providing 1–2 images per month. Considering the influence of seasonal variations, monthly variations of the Tuosu Lake surface area in 2003 and 2020 were also extracted (Figure 2), and it showed that the seasonal variation had only a slight disturbance to the annual trend of lake surface area (see Section 4.1 for details). To observe the lake surface area in more detail, this study selected 20 remote sensing images of the Delingha region from 2000 to 2020 and extracted changes in the surface areas in Tuosu, Keluke, and Gahai Lakes. As optical images are significantly affected by weather conditions, particularly clouds, satellite images were typically only selected from July to August. This is because the summer in Qaidam Basin is dry and sunny with minimal clouds. If no images were available, we substituted images from adjacent months. The data sources used in the study are listed in Table 1. It should be noted that there was a lack of images available in 2012.

Figure 2. Changes in the surface area of Tuosu Lake in 2003 and 2020. Black error bar represents the uncertainty of the extracted lake surface area.

Table 1. Sources of remote sensing data used in this study.

Index	Time	Data Source	Index	Time	Data Source
1	26 May 2000	Landsat 5(TM)	11	2010/7/27	Landsat 5(TM)
2	2 July 2001	Landsat 5(TM)	12	2011/7/14	Landsat 5(TM)
3	5 July 2002	Landsat 5(TM)	13	2013/6/1	Landsat 8(OLI)
4	10 September 2003	Landsat 5(TM)	14	2014/8/23	Landsat 8(OLI)
5	27 August 2004	Landsat 5(TM)	15	2015/8/10	Landsat 8(OLI)
6	13 July 2005	Landsat 5(TM)	16	2016/9/29	Landsat 8(OLI)
7	1 August 2006	Landsat 5(TM)	17	2017/7/14	Landsat 8(OLI)
8	21 September 2007	Landsat 5(TM)	18	2018/10/5	Landsat 8(OLI)
9	5 July 2008	Landsat 5(TM)	19	2019/5/1	Landsat 8(OLI)
10	9 August 2009	Landsat 5(TM)	20	2020/10/10	Landsat 8(OLI)

Uncertainty in the extracted lake surface area mainly originates from the positioning accuracy and indistinguishable mixed pixels in the image [26]. According to previous studies, the registration error is 6 m for TM images [27] and 5 m for OLI images [28]. Considering the registration error, the positioning accuracy in the image, and the clarity of the lake boundary, the uncertainty in the lake surface area was estimated by Equation (1) [29] and is shown as error bars in Figure 3a. Here, E_A is the uncertainty in the extracted lake surface area; l is the length of the lake boundary; LRE_{year} is the resolution error of Landsat images in different years, which should be half the resolution of the image pixel; and E_{co} is the registration error in the image:

$$E_A = l \times \sqrt{LRE_{year}^2 + E_{co}^2} \tag{1}$$

Because of a lack of detailed bathymetric maps of the lakes, the change in lake storage was estimated based on the lake surface area and the slope of the lakeshore zone. The change in water storage between the two stages can be approximated as a frustum, and its volume can be estimated by the following equation [30]:
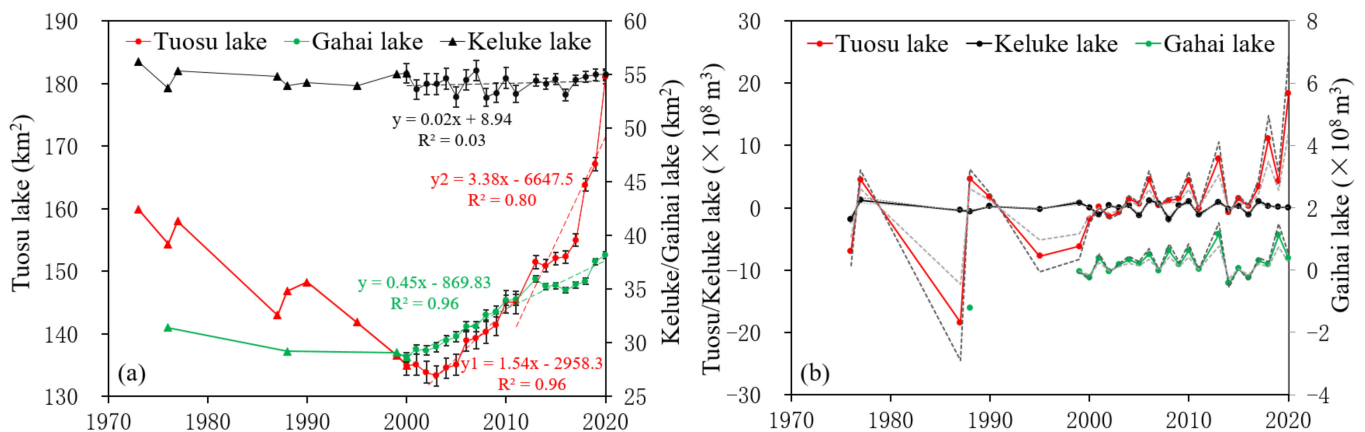
$$\Delta V = \frac{1}{3} \times \left(S_1 + S_2 + \sqrt{S_1 \times S_2} \right) \times H \tag{2}$$

where S_1 and S_2 are the lake surface area in the two stages; ΔV is the change in lake storage; and H is the lake water level interval. The lakes in the study area are located at the end of the alluvial lacustrine plain, with gentle topography and a lakeshore slope of less than 5%, where the slope $I = H/L$, and L is the horizontal distance. For H, the shapes of Tuosu,

Keluk, and Gahai Lakes are approximately equilateral triangles, whose side lengths can be calculated according to the lake surface area in different periods:

$$H = \frac{2}{3} \times I \times \left(\sqrt{S_2} - \sqrt{S_1} \right) \tag{3}$$

here, slope values of 4, 3, and 2 were used to calculate the change in lake water storage, and the calculation results are shown in Figure 3b.

Figure 3. (**a**) Plot depicting the change of lake surface area in the study region extracted from Landsat satellite images. Triangles (before 2000) represent data in the literature [31,32]. y, y1, and y2 represent the least square fitting line of the surface area in Gahai Lake after 2000, Tuosu Lake from 2003 to 2011, and after 2011, respectively. Black error bar represents the uncertainty of the extracted lake surface area. (**b**) Calculated change in lake storage (ΔV). The solid line, dashed lines in dark gray and light gray are the calculation results when the slope (I) is 3, 2, and 4, respectively.

3.2. Hydrological and Meteorological Monitoring Data

The meteorological monitoring network in the alpine region is sparse; however, the single weather station is generally considered to represent the climatic conditions of the basin. The distance between Delingha station (97°22′E, 37°22′N) and Tuosu, Keluke, and Gahai Lakes is only 42, 41, and 27 km, respectively. The terrain between the weather station and the lakes is flat, with no obstruction from mountains, and the climate conditions exhibit minimal spatial variability. Therefore, data from Delingha station were used to represent the climatic conditions near the lakes. Meteorological data at Delingha station were downloaded from the National Meteorological Data Center (http://data.cma.cn/, accessed on 9 August 2021); this included daily data of relative humidity, minimum relative humidity, mean temperature, maximum temperature, minimum temperature, mean wind speed, minimum wind speed, and annual precipitation. Delingha station lacks solar radiation data; therefore, these data were replaced by monitoring data from the nearest station in Golmud (94°54′E, 36°25′N).

Runoff data from Delingha station (1957–2018) and Zelinggou station (1957–1983) were compiled from the *Hydrological Yearbook*. Lake water temperature data for Tuosu, Keluke, and Gahai Lakes were obtained from a dataset of daily lake surface temperature over the Tibetan Plateau (1978–2017) compiled by the National Tibetan Plateau Data Center (http://data.tpdc.ac.cn, accessed on 11 August 2021) [33], which uses the improved lake water temperature model (air2water) to simulate the annual surface temperature every day. Considering the different available periods of sequences, the calculation interval for analyzing lake evaporation was 1984–2016 in this study.

3.3. Penman–Monteith Model

Accurate quantification of lake evaporation is essential for determining the water budget of a lake, especially for endorheic lakes, where evaporation is the most important

output term of the lake water budget [34–36]. Based on the energy conservation formula, Penman [37] first proposed the Penman formula for calculating evapotranspiration, from which many water surface evaporation models have been developed [38,39]. After comparing 14 evaporation models with baseline Bowen ratio energy budget measurements, Rosenberry [40] identified that the De BruinKeijman, Priestley Taylor, and Penman models provided the best estimates of water surface evaporation. McJannet then compared eddy covariance measurements with the De BruinKeijman, Priestley Taylor, and Penman–Monteith models, [15,16] and found that the Penman–Monteith model was most suitable for water surface evaporation because it considers both the vapor pressure gradient and wind speed, and produced estimates of total evaporation that varied from the actual measurements by less than 1%. In addition, the Penman–Monteith model has been improved by proposing the general application of wind functions, making it applicable for calculating evaporation for water bodies ranging from tens to hundreds of kilometers. This improved Penman–Monteith model has been applied in several subsequent studies [17–19].

In this study, we used the improved Penman–Monteith model to calculate lake surface evaporation (see McJannet [15,16] for details). Uncertainty in the evaporation value mainly derived from data measurement and parameter calculation. The measurement error comes from the measurement of wind speed, temperature, humidity, and accumulated solar radiation. These errors are inevitable but have little impact on the final calculation results.

3.4. Sampling and Isotope Measurements

Hydrogen (^{2}H) and oxygen (^{18}O) isotopes are widely used to study hydrological cycles [41,42] and qualitatively identify water sources and trace groundwater runoff processes [11,13]. In this study, 47 water samples were collected from rivers, phreatic groundwater, confined groundwater, springs, and lakes (Figure 1). River water samples (R07, R09, and R12) were collected from the upper reaches of Bayin River, close to where the river exits the mountains, mainly from glacial meltwater; thus, they are minimally influenced by precipitation and groundwater. These three samples represent the hydrogen (^{2}H) and oxygen (^{18}O) isotope characteristics of glacial meltwater. In this study, only one lake water sample was collected from Keluke Lake, which was analyzed together with 12 lake water samples collected from Yang Lake [11], which are discussed in Section 4.4.

Stable isotopes of hydrogen and oxygen (^{2}H, ^{3}H, ^{18}O) were measured at the State Key Laboratory of Hydrology, Water Resources, and Hydraulic Engineering, Hohai University. ^{18}O/^{16}O and ^{2}H/^{1}H ratios were measured using a MAT253 mass spectrometer. The isotope ratio 'δ' was expressed as follows:

$$\delta_{sample}(‰) = \left(R_{sample}/R_{standard} - 1 \right) \times 1000 \tag{4}$$

where R_{sample} and $R_{standard}$ are the isotope ratios (^{18}O/^{16}O, ^{2}H/^{1}H) of the sample and standard, respectively, and the international standard is the δ^2H and δ^{18}O of Vienna mean seawater. The measurement errors of δ^{18}O and δ^2H were ±0.1‰ and ±1‰, respectively. The tritium content of samples was measured by a liquid scintillation meter (TRI-CARB 3170 TR/SL) with a detection limit of 0.2 TU and precision of >0.8 TU. The measurement results for hydrogen (^{2}H, ^{3}H) and oxygen (^{18}O) isotopes are shown in Table 2.

Table 2. Isotope measurement results (^{2}H, ^{18}O, and tritium) for different water samples in the study area.

Sam. No.	Type	Latitude (N)	Longitude (E)	Depth (m)	δ^2H (‰)	δ^{18}O (‰)	^{3}H (TU)
R01	RW	37°23′15″	97°21′39″		−58.6	−8.81	14.0
R02	RW	37°23′43″	97°22′04″		−58.4	−8.76	
R03	RW	37°23′55″	97°21′35″		−52.1	−7.34	
R07	RW	37°22′38″	97°26′40″		−57.1	−6.60	
R09	RW	37°21′06″	97°33′12″		−56.9	−8.82	17.8
R10	RW	37°21′11″	97°37′31″		−58.4	−8.97	11.6
R12	RW	37°23′03″	97°42′34″		−56.7	−8.63	16.7
R22	RW	37°19′06″	97°21′59″		−57.4	−8.77	
R25	RW	37°11′44″	97°20′21″		−56.3	−8.80	
R31	RW	37°09′21″	97°17′56″		−56.1	−8.39	
R33	RW	37°9′39″	97°10′58″		−56.3	−8.49	
R36	RW	37°15′07″	97°02′14″		−50.8	−7.20	
R39	RW	37°32′47″	96°50′03″		−59.6	−9.23	
R40	RW	37°32′47″	96°50′03″		−59.8	−9.26	
R41	RW	37°41′14″	96°31′03″		−53.6	−7.59	
R43	RW	37°36′31″	96°51′35″		−59.8	−9.44	
R47	RW	37°22′38″	97°20′37″		−60.1	−9.34	
L37	LW	37°18′56″	96°54′07″		−46.1	−6.42	
L42	LW	37°43′32″	96°28′43″		−22.1	−1.05	
G17	SW	37°12′20″	97°24′02″		−58.3	−8.82	11.2
G18	SW	37°13′10″	97°27′36″		−60.0	−9.16	11.9
G20	SW	37°13′24″	97°29′24″		−62.4	−9.38	5.0
G35	SW	37°15′08″	97°02′12″		−66.6	−10.08	3.7
G26	PGW	37°12′07″	97°17′54″	0.26	−58.2	−8.89	9.0
G19	PGW	37°13′07″	97°27′35″	0.6	−57.8	−8.68	
G27	PGW	37°12′18″	97°16′14″	1.2	−60.0	−9.08	
G24	PGW	37°12′38″	97°20′20″	1.4	−62.5	−9.36	
G16	PGW	37°13′24″	97°25′08″	1.9	−60.5	−8.82	9.1
G08	PGW	37°22′33″	97°27′16″	2.0	−42.0		
G28	PGW	37°13′05″	97°14′11″	3.5	−58.7	−9.19	
G05	PGW	37°22′40″	97°26′00″	3.8	−62.2	−9.39	15.1
G45	PGW	37°20′59″	96°46′32″	26.4	−53.6	−8.31	
G44	PGW	37°21′00″	96°46′25″	27.6	−50.8	−8.26	11.8
G29	PGW	37°15′46″	97°13′12″	12.0	−64.8	−9.92	5.5
G30	PGW	37°17′55″	97°12′47″	14.9	−62.5	−9.56	
G34	PGW	37°19′05″	97°12′36″	18.2	−58.8	−8.88	9.6
G06	PGW	37°22′44″	97°25′54″	20.0	−65.4	−9.28	
G23	CGW	37°17′02″	97°20′28″	31.8	−58.9	−8.84	10.9
G15	CGW	37°17′23″	97°24′07″	40.4	−60.3	−9.08	
G11	CGW	37°21′14″	97°40′20″	50.0	−71.1	−10.60	1.3
G14	CGW	37°19′31″	97°23′49″	63.3	−58.2	−8.86	
G04	CGW	37°22′45″	97°25′51″	65.0	−60.4	−9.08	15.6

Note: PGW, CGW, RW, SW, and LW represent phreatic water, confined water, river water, spring water, and lake water, respectively.

4. Results

4.1. Long-Term Changes in Lake Surface Area

Lakes generally have seasonal variations, which possibly affect the interannual trend analysis of change in the lake surface area. Considering this effect of seasonal variations, the monthly variations of the Tuosu Lake surface area in 2003 and 2020 were extracted (Figure 2). The results show that the lake surface areas of Tuosu Lake in 2003 and 2020 were 128.2–136.1 km^2 and 174.0–178.7 km^2 with uncertainties within 1.6% and 1.2%, respectively. This indicates that the extracted lake surface areas are reliable. The maximum differences of lake surface area caused by seasonal variation are 7.9 km^2 and 4.7 km^2 in 2003 and 2020, respectively, and the relative deviation is within 4% and 2%, respectively. Therefore, the seasonal variation has only a slight effect on the interannual trend of the lake surface area.
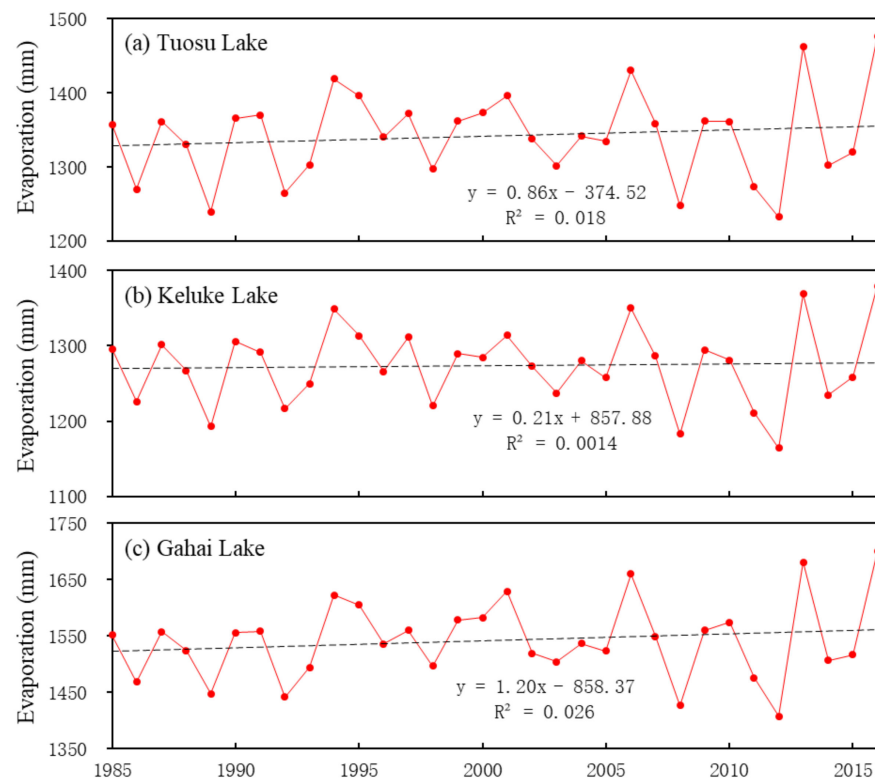
Changes in the surface areas of Tuosu, Keluke, and Gahai Lakes from 2000 to 2020, as well as changes in lake water storage calculated from the lake surface area and slope (I = 2, 3, and 4), are shown in Figure 3a,b, respectively. The average surface areas of Keluke, Tuosu, and Gahai Lakes were 54.2, 146.5, and 33.1 km^2, with uncertainties of within 1.3%, 1.7%, and 1.6%, respectively. Keluke Lake remained stable because it is connected to Tuosu Lake through the Lianshui River. When the water level of Keluke Lake rises, excess water flows into Tuosu Lake through the river. Therefore, changes in lake surface area mainly occurred in Tuosu Lake, with three distinct trends: continuous shrinkage (before 2003), slow expansion (2003–2011), and rapid expansion (after 2011). Before 2003, Tuosu Lake shrank at a rate of 2.50 km^2/year and then gradually increased at a rate of 1.54 km^2/year from 2003 to 2011, with an average increase in lake water storage of 1.45 $\times$ 10^8 m^3/year (Figure 3b). After 2011, Tuosu Lake expanded rapidly at a rate of up to 3.38 km^2/year, which was much higher than the overall increase of 2.19 km^2/year (R^2 = 0.88) after 2003. At this time, the average increase in lake water storage was as high as 5.75 $\times$ 10^8 m^3/year (I = 3). Gahai Lake shrank gradually prior to 2000 and then expanded steadily after 2000 at a rate of 0.45 km^2/year (R^2 = 0.96), with an average increase in lake water storage of 0.29 $\times$ 10^8 m^3/year. Although detailed lakeshore slopes were not obtained in the calculation of lake water storage changes, the gentle lakeshore zone allowed changes in water storage to be largely reflected in the lake surface area rather than the lake height, which supports our subsequent analysis of the water budget based on surface area changes.

Similar lake expansion occurred at the edge of the Tibetan Plateau. Taitema Lake in the north of the Altun Mountains reappeared in 2003 after prolonged drying over many years, and then expanded rapidly [43]. Similarly, Qinghai Lake in the northeast margin of the Tibetan Plateau expanded rapidly at a rate of 8.67 km^2/year after 2003 (https://hydroweb.theia-land.fr/hydroweb, accessed on 27 November 2021), with a simultaneous increase in groundwater level in the Hexi corridor in the north of the Qilian Mountains [44], which may imply similar lake response patterns.

4.2. Lake Evaporation Calculated by the Improved Penman–Monteith Model

Lake expansion is a direct reflection of the water budget of a lake. Regional groundwater head distribution determines groundwater inflow and groundwater outflow in the water balance of the endorheic lake. The groundwater level in the study area gradually decreases from the mountains to the plains, and the groundwater flows from the mountains to the lakes and eventually contributes to the lakes. For endorheic lakes, the input components of the lake water budget mainly include precipitation, runoff, and groundwater inflow, while the output component is mainly lake evaporation, and groundwater outflow can be neglected. In this study, lake evaporation was quantified by using the improved Penman–Monteith model and used to analyze the influence of the major output component (lake evaporation) on lake expansion in the study area. Based on the monitoring data of Delingha station, evaporation values for Tuosu, Keluke, and Gahai Lakes were 1233–1476 mm/year, 1164–1379 mm/year, and 1407–1700 mm/year, with average values of 1342, 1274, and 1542 mm/year, respectively (Figure 4). These results show that evaporation varied significantly between lakes with different lake surface areas and depths. All three lakes exhibited stable interannual evaporation values, with insignificant variation trends and relative deviations of 9.9%, 9.6%, and 10.2%, respectively. Therefore, evaporation did not cause significant changes in lake surface area and cannot explain the rapid expansion of the lakes since 2003. This suggests that climate change processes such as increased temperature and precipitation did not significantly affect lake evaporation and were not the main factors affecting the lake water budget during the study period.

Figure 4. Plots exhibiting the evaporation of Tuosu (**a**), Keluke (**b**), and Gahai Lakes (**c**) calculated by the improved Penman–Monteith model.
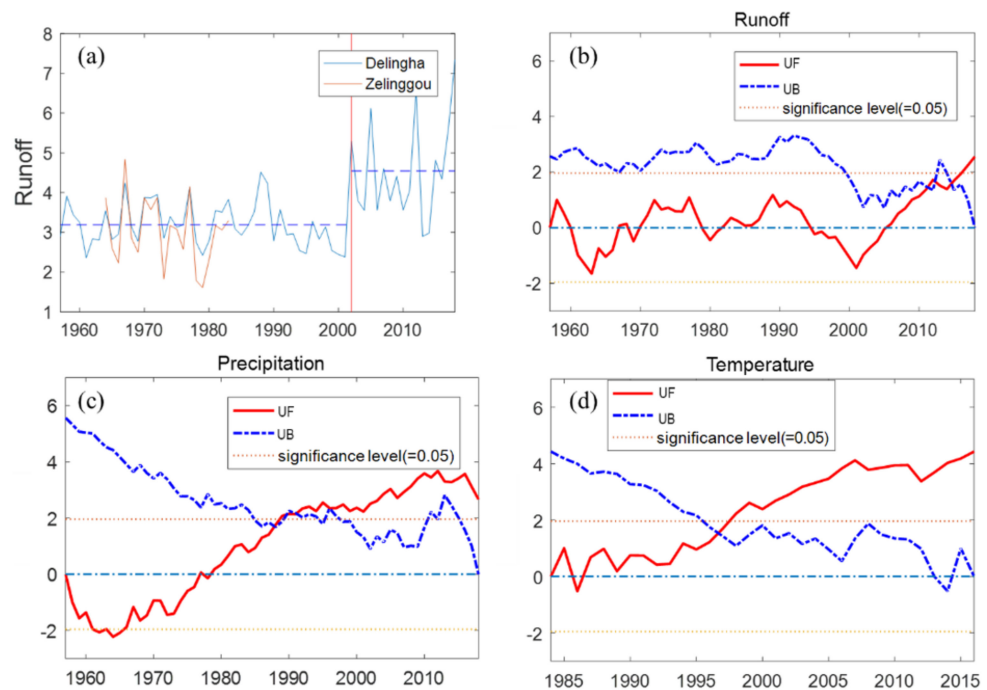
4.3. Annual Hydrometeorological Trends

Considering the lack of significant changes in the main output component of the lake water budget (lake evaporation), rapid lake expansion may instead have been caused by the input components, which include precipitation, runoff, and groundwater inflow. Rainfall and runoff data were derived from long-term monitoring at Delingha meteorological and hydrological stations. Because of the complexity and hidden nature of the groundwater runoff process, the groundwater contribution to lakes is difficult to directly quantify and observe long-term. Therefore, we first analyzed the long-term variation trends of rainfall and runoff.
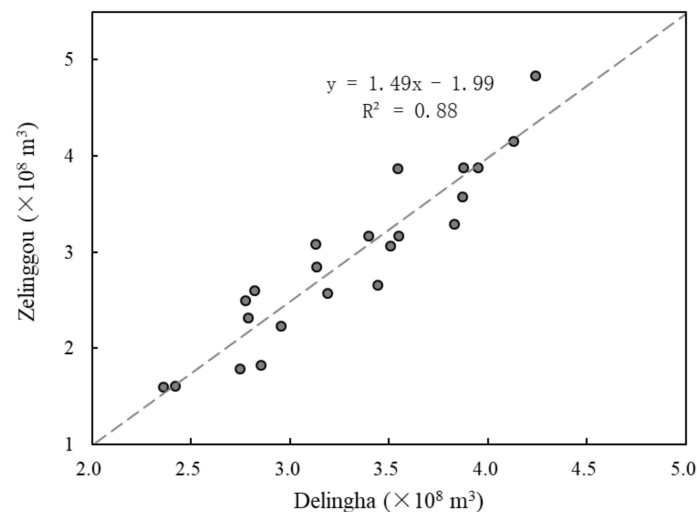
The Mann–Kendall test was used to inspect the long-term trends of hydrometeorological data and identify abrupt changes in the time-series data. An abrupt change in the precipitation time-series occurred in 1989 ($\alpha = 0.05$), with average precipitation before and after this change equal to 156 mm/year and 215 mm/year, respectively, representing an increase of more than 37.7%. However, this abrupt change in precipitation occurred much earlier than the beginning of lake expansion in 2003. This indicates that, although precipitation increased annually, it was not the dominant factor influencing lake expansion. Additionally, precipitation in the plain area is only 50 mm/year; thus, its contribution to the lake water budget can be neglected (Comprehensive Investigation Committee of Chinese Academy of Sciences, 1984).

Conversely, there was no obvious abrupt change in the runoff measured at Delingha station, although there was a significant difference in average runoff before and after 2002 (3.19×10^8 m^3/year and 4.55×10^8 m^3/year, respectively), representing a difference of 42.6% (Figure 5b). Runoff from Zelinggou station represents glacier meltwater, whereas Delingha station is located at the boundary between the upper and middle reaches of the Bayin River; thus, runoff is derived from both glacier meltwater and precipitation in mountainous areas. A comparison of the runoff values between the two stations during 1957–1983 revealed strong similarity, with a correlation coefficient of up to 0.88 (Figure 6). Runoff at Zelinggou station accounts for 90% of that at Delingha station, which indicates

that glacial meltwater is the main source of the Bayin River. The rate of glacial melt is controlled by the average air temperature, which changed significantly ($\alpha = 0.05$) in 1997, from 4.1 °C to 5.1 °C, representing an increase of 23.3% (Figure 5d). This increase in air temperature likely accelerated glacier meltwater.

Figure 5. Plots depicting the change of runoff at Delingha and Zelinggou stations (**a**), results of MK test for runoff (**b**), precipitation (**c**), and temperature (**d**) at Delingha station.
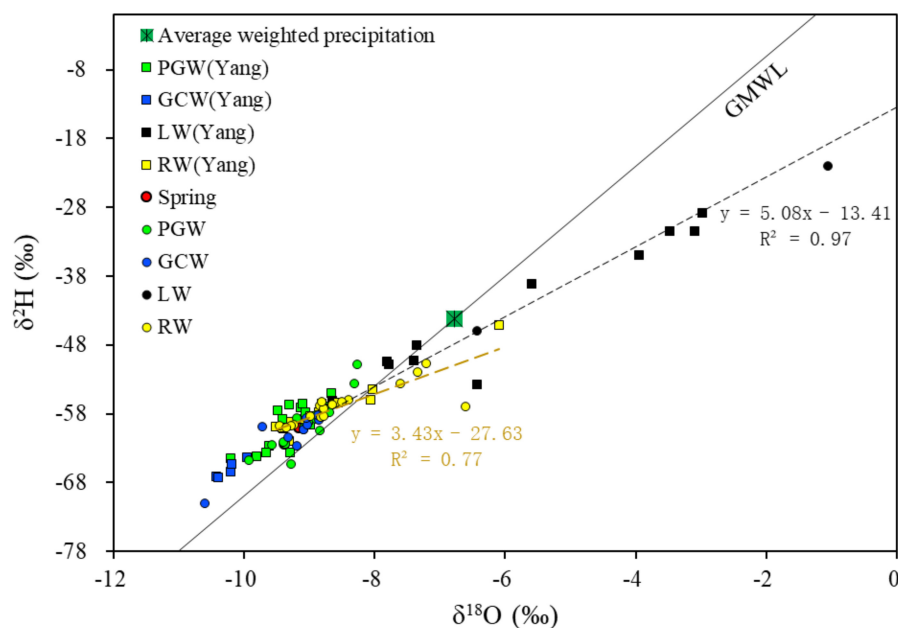

Figure 6. Graph representing the comparison between runoff at Delingha and Zelinggou stations from 1957 to 1983.

4.4. Isotopic Characteristics of Surface Water, Groundwater, and Spring Water

To trace groundwater processes and sources, the stable isotopes (^{2}H, ^{18}O) of collected water samples were analyzed (Figure 7 and Table 2). Samples R12, R09, and R07 represent glacial meltwater, as discussed earlier. The δ^2H and δ^{18}O of glacial meltwater, phreatic groundwater, and river water lie in the range of −57.1 to −56.7‰ and −8.8 to −6.6‰, −65.4 to −42.0‰ and −9.9 to −8.3‰, and −60.1 to −50.8‰ and −9.4 to −6.6‰, respectively. The points of river water were distributed along with the least square fitting line in Figure 7,

i.e., $\delta^2H = 3.43\ \delta^{18}O -27.63$ ($R^2 = 0.77$), showing the evaporation characteristics of river water. Most of the river points fell within the range of phreatic groundwater. This implies a strong interaction between river water and phreatic groundwater and that the river was recharged by both phreatic groundwater and glacial meltwater. The fitting line of lake water was $\delta^2H = 5.1883\ \delta^{18}O - 12.599$ ($R^2 = 0.81$), and its intersection ($-54.7‰$, $-8.1‰$) with the global meteoric water line (GWML) fell within the range of river water, suggesting that phreatic groundwater contributed to the lake after flowing into the river.

Figure 7. Plot illustrating $\delta^{18}O$ vs. δ^2H diagram of groundwater, lake water, river water, and spring water in the study area of the Qaidam Basin, China. Squares represent samples from the literature [11].

Zhang [45] also collected precipitation samples from Delingha from September 1991 to December 1992 and derived a weighted average of δ^2H and $\delta^{18}O$ in precipitation of $-44.2‰$ and $-6.8‰$, respectively. The δ^2H and $\delta^{18}O$ values of confined groundwater ranged from $-71.1‰$ to $-58.2‰$ and from $-10.6‰$ to $-8.8‰$, respectively. Thus, the confined groundwater was more depleted in deuterium and oxygen-18 than phreatic groundwater and local meteoric precipitation. The concentrations of tritium in river water, spring water, and confined water were 11.6–17.8 TU, 3.7–11.9 TU, and 1.3–15.6 TU, respectively.

5. Discussion

5.1. Potential Causes of Lake Expansion

Long-term changes in the surface areas of Tuosu, Keluke, and Gahai Lakes during the study period were the result of a combination of climate change and groundwater contributions, with climate change processes mainly including increased precipitation and temperature. Expansion of Tuosu Lake was particularly obvious; hence, we used this lake as an example to analyze the reasons for lake expansion. Long-term lake evaporation was stable at 1342 mm/year, indicating that increased temperatures affect the lake surface area by accelerating glacier melting rather than promoting lake evaporation. According to long-term meteorological data, lake evaporation and runoff remained stable prior to 2003, whereas precipitation slowly increased (2.279 mm/year). However, the surface area of Tuosu Lake decreased from 159.9 km^2 in 1973 to 132.3 km^2 in 2003; thus, lake shrinkage was likely caused by the decrease in the groundwater contribution to the lake.

From 2003 to 2011, temperature and precipitation increased by 18.6% and 34.1%, respectively (Table 3), which caused an increase in runoff of 1.21×10^8 m^3/year and 0.15×10^8 m^3/year at Delingha station, respectively. Temperature increases during this period mainly promoted lake expansion by accelerating glacial melting, which resulted

in more surface runoff into the lake. This reflects the contribution of glacial meltwater to lake expansion. The rates of temperature, precipitation, and runoff increase were similar between the two periods of 2003–2011 and 2011–present; however, the expansion rate of Tuosu Lake increased rapidly between these periods, from 1.22 km^2/year to 3.38 km^2/year. Thus, the increase in runoff caused by accelerated glacial melting cannot fully explain the observed lake expansion, which implies that groundwater was an important reason for rapid lake expansion.

Table 3. Variation of factors affecting the Tuosu Lake surface area before 2003 and after 2003.

	Time	Runoff	Precipitation	Temperature	Evaporation	Lake Surface Area
Average	Before 2003	3.2	171	4.3	1341.8	148.6
	After 2003	4.5	229	5.1	1343.0	146.5
Variation	Whole time	1.3	58	0.8	1.1	−2.1
Variation ratio	Whole time	40.6%	34.1%	18.6%	0.09%	−1.4%
Variation rate	Before 2003	−0.002	2.279	0.068	3.087	−0.867
	After 2003	0.092	−0.777	0.034	3.080	2.190
	Whole time	0.024	2.083	0.051	0.858	0.131

Note: units of runoff, precipitation, evaporation, and lake surface area are 10^8 m^3/year, mm/year, mm/year, and km^2, respectively.

When glacial meltwater flows through the piedmont plain, some infiltrates the ground as subsurface runoff, which is an important contributor of water to the lake. However, not all of the groundwater contribution to the lakes is derived from glacial meltwater, as groundwater collected near the lakes showed greater isotopic depletion than glacial meltwater in the basin. This indicates the existence of other water sources with more depleted isotopes, which may be related to the mechanism of rapid lake expansion. Several earlier studies have revealed the important role of groundwater in lake expansion and shrinkage [8–11]. For example, the groundwater contribution flux estimated by the radon isotope (^{222}Rn) is $0.55 - 2.49 \times 10^{-4}$ m^3/(s × m); however, this flux was only measured at a certain time [11]. In future studies, long-term observations of groundwater contributions are required to determine and predict the effects of groundwater on lakes.

5.2. Sources of Groundwater Contribution to Lakes

Deuterium and oxygen-18 isotopes revealed that confined groundwater is characterized by significant isotopic depletion. The origin of depleted confined groundwater in alpine arid basins is controversial. According to ^{14}C-dating of groundwater, it is generally believed that glacial meltwater generated a large amount of recharge after the last glacial period [46,47], or some studies have suggested that meteoric precipitation during glacial and interglacial periods recharged the confined groundwater [48–50]. ^{14}C-dating of groundwater age strictly requires that endogenous CO_2 from no other sources is dissolved in the groundwater system, which can dilute the ^{14}C concentration in the groundwater, resulting in overestimation of the significant groundwater age. However, Qaidam Basin is an active geological environment containing multiple crisscrossing fractures. Thus, mantle-derived endogenous CO_2 with low ^{14}C activity can migrate upward through active structures such as fault zones and dissolve into the groundwater, leading to significant overestimation of groundwater age [51,52] by tens of thousands of years. As such, tritium was used to identify the groundwater renewal cycle in this study. The half-life of tritium is only 12.3 a, and the background value of tritium in natural groundwater systems is generally less than 1 TU. After 1952, global nuclear explosion tests caused a peak in the atmospheric tritium concentration. Therefore, groundwater systems with tritium values >5 TU are considered to have a groundwater renewal cycle of several decades. The confined groundwater samples in this study exhibited high tritium concentrations of between 8.5 TU and 15.6 TU, which demonstrates that confined groundwater is rapidly circulated and recharged by modern water since the global nuclear explosion tests. Therefore, confined groundwater in the

study area may be recharged by water sources with more depleted isotopic signatures from other areas.

Previous research [12] has revealed an enormous amount of missing water in Qiangtang Basin, with a leakage water volume of up to 540×10^8 m^3/year, which is related to tectonic activity such as earthquakes. Leakage occurs in six major rift valleys in the southern part of Qiangtang Basin and is transported to other basins by underground runoff. Although the drainage area was not identified in previous literature, this leakage was likely discharged to surrounding areas at lower elevations, causing groundwater levels to rise and lakes to expand. Delingha, Qinghai Lake, Taklamakan Desert, and Hexi Corridor, located on the northern edge of the Tibetan Plateau, have a relatively low altitude and an active geological environment with frequent earthquakes, providing suitable conditions for the remote discharge of groundwater. Moreover, earthquakes are known to increase groundwater discharge [53–55]. In 2003, groundwater release induced by earthquakes was observed in Qinghai Lake (https://hydroweb.theia-land.fr/hydroweb, accessed on 27 November 2021), Taklimakan Desert [43], and the Hexi corridor [44], resulting in the emergence of new lakes, the expansion of existing lakes, and an increase in groundwater levels. An earthquake with a magnitude of 6.1 can affect areas as far as 80 km from the earthquake source [56]. The 2003 M$_s$ 6.4 earthquake that occurred in the northwestern part of the study area (Figure 1) was only 57 km away from Tuosu Lake; thus, it very likely led to an increase in groundwater contribution to the lake. The endorheic lakes in the study area represent places of convergence for surface water and groundwater, and stable isotope analysis showed that groundwater is an important contributor to the lakes. Outflow from the lake to groundwater is limited, which in turn supports that lake evaporation is the main output of lake water balance. The distinctly depleted H and O isotopes in the confined groundwater indicate remote discharge from a high-altitude water source with a more depleted isotopic signature. Therefore, it is speculated that either the 2003 M$_s$ 6.4 earthquake in the northwest of Delingha or the 2001 M$_s$ 8.1 earthquake in the Kunlun Mountains were possible mechanisms for expansion of the lakes in the study area. Earthquakes enhance crustal permeability and keep fractures open [43,44], which promotes the groundwater contribution to lakes and in turn causes rapid lake expansion.

5.3. Uncertainty in Lake Evaporation Calculations

Uncertainty in the calculated evaporation values is derived from the lack of solar radiation monitoring data at the Delingha station, which was replaced by data from the nearby Golmud station in this study. Because the intensity of solar radiation is mainly related to latitude, and the latitude difference between Delingha and Golmud stations is only approximately 1°, the uncertainty caused by solar radiation data can be ignored. Uncertainty also originates from the lake surface temperature simulated by the improved lake water temperature model (air2water), with a deviation of ± 0.55 °C, which also has a limited impact on the calculation results. Combined with remote sensing and meteorological data, evaporation from Tuosu Lake is 1333 mm/year [57], which only differs by 0.7% from the value calculated in this study. Earlier studies have reported substantial variation in evaporation between lakes, even if the lake surface areas are similar. For example, Laguo and Yang Lakes have only a 1.3% difference in surface area but a 24.4% difference in lake evaporation [57]. The improved Penman–Monteith model considers the effect of lake surface area and depth on evaporation, leading to more accurate calculation results.

5.4. Mitigating the Environmental Effects of Lake Expansion

Lake expansion likely affects the groundwater runoff process, leading to geological and environmental problems. For example, Gahai Lake is located at the southeastern edge of the alluvial fan and has no inflow from surface runoff. Water from the Bayin River seeps into groundwater in the middle reaches, with weak groundwater runoff in the southeast direction being one of the sources of Gahai Lake. The Gahai irrigation area (D) is located in this groundwater flow path (Figure 8). The geological formation in front of the alluvial

fan is mainly composed of fine-grained sediment, which has a strong water-blocking effect. The water level of Gahai Lake has been rising continuously since 2000, which slows down the groundwater discharge rate and enhances groundwater level rises in the surrounding area. After 2006, the groundwater level increased at a rate of 0.5 m/year. In 2012, the groundwater level came close to the surface and overflowed, rising as high as 11 m in some areas [58]. This directly led to problems such as foundation collapses, and soil salinization occurred in the vicinity of Gahai Lake, which threatened the lives and livelihoods of nearby residents. Therefore, measures should be taken to mitigate the effects of lake expansion in the study area.

Figure 8. The distribution of irrigation area in Delingha. A, B, C, D, F represents Huaitoutala, Gebi, Delingha, Gahai, and Zelinggou irrigation area, respectively. The blue arrow represents the direction of weak groundwater runoff after the Bayan River leakage.

Furthermore, when the water level of Keluke Lake rises, the water can be discharged to Tuosu Lake through the Lianshui River. The Huaitoutala irrigation area (A) and nearby villages are located northwest of Keluke Lake (Figure 8), at higher elevation than both Keluke Lake (by 36 m) and Tuosu Lake (by 48 m). Therefore, the future expansion of Tuosu Lake will have little impact on the nearby irrigation areas and villages but is likely to promote expansion of the marsh in the northeast of Tuosu Lake. Considering the long-term trend of climate warming, a rise in groundwater levels in the vicinity of Gahai Lake is inevitable. Therefore, to ensure the safety of residents and continued operation of the irrigation area, drainage channels can be excavated at the end of the alluvial fan to divert groundwater to the Bayin River. Despite the potential for further increases in the water level of Tuosu Lake after channel excavation, the lack of villages and farmland around the lake makes this an appropriate management solution.

6. Conclusions

Remote sensing techniques, model calculations, and statistical analyses were used to analyze lake surface area changes in response to climate change and groundwater in Qaidam Basin, and stale isotopes were used to identify potential sources of groundwater. Our analysis suggests that long-term increases in temperature and precipitation had a certain promotion effect on lake expansion, with higher temperatures accelerating glacier melting rather than promoting lake evaporation. However, the significant increase in the rate of lake expansion also indicated the important contribution of groundwater to lake expansion, which includes not only glacial meltwater that infiltrates the piedmont plain but also other sources of water. Isotope data revealed that confined groundwater can circulate rapidly and is recharged by modern water since the global nuclear explosion tests. The more depleted isotopic signature of the confined groundwater compared to that of local

meteoric precipitation and glacial meltwater suggested recharge by water sources with more isotopic depletion from other basins. Therefore, it is speculated that the 2003 M_s 6.4 earthquake in the northwest of Delingha may be a possible mechanism for the expansion of the lakes in the study area by enhancing crustal permeability and keeping fractures open, which promotes the groundwater contribution to lakes and in turn causes rapid lake expansion and increased groundwater levels.

The expansion of Gahai Lake has caused an increase in surrounding groundwater levels, which threatens the lives and livelihoods of residents. Under the long-term trend of climate warming, Gahai Lake will inevitably continue to expand in the future. Therefore, to ensure the safety of residents and continued operation of the irrigation area, it is suggested that drainage channels can be excavated at the end of the alluvial fan to divert groundwater to the Bayin River and eventually Tuosu Lake. This study emphasizes the important role of groundwater in lake expansion and improves our understanding of groundwater sources, circulation, and evolution patterns in Qaidam Basin and the arid area of northwest China. Currently, the future contribution of groundwater to lake expansion cannot be predicted because of a lack of groundwater monitoring data in the study area; therefore, future work should include long-term monitoring of the groundwater contribution to lakes in Qaidam Basin.

Author Contributions: Conceptualization, J.C. (Jiaqi Chen) and X.Z.; methodology, X.Z.; investigation, X.Z. and F.M.; writing—original draft preparation, X.Z.; writing—review and editing, J.C. (Jiaqi Chen), J.C. (Jiansheng Chen), and T.W.; supervision, J.C. (Jiansheng Chen). All authors have read and agreed to the published version of the manuscript.

Institutional Review Board Statement: Not applicable.

Informed Consent Statement: Not applicable.

Data Availability Statement: Not applicable.

Conflicts of Interest: The authors declare no conflict of interest.

References

1. Yang, K.; Wang, J.; Lei, Y.; Chen, Y.; Zhu, L.; Ding, B.; Qin, J. Quantifying evaporation and its decadal change for Lake Nam Co, central Tibetan Plateau. *J. Geophys. Res. Atmos.* **2016**, *121*, 7578–7591. [CrossRef]
2. Wang, X.; Gong, P.; Zhao, Y.; Xu, Y.; Cheng, X.; Niu, Z.; Luo, Z.; Huang, H.; Sun, F.; Li, X. Water-level changes in China's large lakes determined from ICESat/GLAS data. *Remote Sens. Environ.* **2013**, *132*, 131–144. [CrossRef]
3. Zhang, G.; Yao, T.; Xie, H.; Zhang, K.; Zhu, F. Lakes' state and abundance across the Tibetan Plateau. *Chin. Sci. Bull.* **2014**, *59*, 3010–3021. [CrossRef]
4. Zhang, G.; Xie, H.; Kang, S.; Yi, D.; Ackley, S.F. Monitoring lake level changes on the Tibetan Plateau using ICESat altimetry data (2003–2009). *Remote Sens. Environ.* **2011**, *115*, 1733–1742. [CrossRef]
5. Lei, Y.; Yao, T.; Bird, B.W.; Yang, K.; Zhai, J.; Sheng, Y. Coherent lake growth on the central Tibetan Plateau since the 1970s: Characterization and attribution. *J. Hydrol.* **2013**, *483*, 61–67. [CrossRef]
6. Lei, Y.; Yang, K.; Wang, B.; Sheng, Y.; Bird, B.W.; Zhang, G.; Tian, L. Response of inland lake dynamics over the Tibetan Plateau to climate change. *Clim. Change* **2014**, *125*, 281–290. [CrossRef]
7. Song, C.; Huang, B.; Richards, K.; Ke, L.; Phan, V.H. Accelerated lake expansion on the Tibetan Plateau in the 2000s: Induced by glacial melting or other processes? *Water Resour. Res.* **2014**, *50*, 3170–3186. [CrossRef]
8. Li, X.Y.; Xu, H.Y.; Sun, Y.L.; Zhang, D.S.; Yang, Z.P. Lake-level change and water balance analysis at lake Qinghai, West China during recent decades. *Water Resour. Manag.* **2007**, *21*, 1505–1516. [CrossRef]
9. Tan, H.; Zhang, Y.; Rao, W.; Guo, H.; Ta, W.; Lu, S.; Cong, P. Rapid groundwater circulation inferred from temporal water dynamics and isotopes in an arid system. *Hydrol. Process.* **2021**, *35*, e14225. [CrossRef]
10. Wiebe, A.J.; Conant, B.; Rudolph, D.L.; Korkka-Niemi, K. An approach to improve direct runoff estimates and reduce uncertainty in the calculated groundwater component in water balances of large lakes. *J. Hydrol.* **2015**, *531*, 655–670. [CrossRef]

11. Yang, N.; Zhou, P.; Wang, G.; Zhang, B.; Shi, Z.; Liao, F.; Li, B.; Chen, X.; Guo, L.; Dang, X.; et al. Hydrochemical and isotopic interpretation of interactions between surface water and groundwater in Delingha, Northwest China. *J. Hydrol.* **2021**, *598*, 126243. [CrossRef]

12. Yong, B.; Wang, C.Y.; Chen, J.; Chen, J.; Barry, D.A.; Wang, T.; Li, L. Missing water from the Qiangtang Basin on the Tibetan Plateau. *Geology* **2021**, *49*, 867–872. [CrossRef]

13. Wen, G.; Wang, W.; Duan, L.; Gu, X.; Li, Y.; Zhao, J. Quantitatively evaluating exchanging relationship between river water and groundwater in Bayin River Basin of northwest China using hydrochemistry and stable isotope. *Arid Land Geogr.* **2018**, *41*, 734–743.

14. Qin, B.; Qun, H. Evaluation of the climatic change impacts on the inland lake—A case study of Lake Qinghai, China. *Clim. Change* **1998**, *39*, 695–714. [CrossRef]

15. McJannet, D.L.; Cook, F.J.; Burn, S. Comparison of techniques for estimating evaporation from an irrigation water storage. *Water Resour. Res.* **2013**, *49*, 1415–1428. [CrossRef]

16. McJannet, D.L.; Webster, I.T.; Cook, F.J. An area-dependent wind function for estimating open water evaporation using land-based meteorological data. *Environ. Model. Softw.* **2012**, *31*, 76–83. [CrossRef]

17. Rodrigues, I.S.; Costa, C.A.G.; Lima Neto, I.E.; Hopkinson, C. Trends of evaporation in Brazilian tropical reservoirs using remote sensing. *J. Hydrol.* **2021**, *598*, 126473. [CrossRef]

18. Li, W.; Brunner, P.; Hendricks Franssen, H.J.; Li, Z.; Wang, Z.; Zhang, Z.; Wang, W. Potential evaporation dynamics over saturated bare soil and an open water surface. *J. Hydrol.* **2020**, *590*, 125140. [CrossRef]

19. Altho, D.; Neiva, L.; David, D.; Couto, H. Improving methods for estimating small reservoir evaporation in the Brazilian Savanna. *Agric. Water Manag.* **2019**, *216*, 105–112. [CrossRef]

20. Zhang, G.; Yao, T.; Shum, C.K.; Yi, S.; Yang, K.; Xie, H.; Feng, W.; Bolch, T.; Wang, L.; Behrangi, A.; et al. Lake volume and groundwater storage variations in Tibetan Plateau's endorheic basin. *Geophys. Res. Lett.* **2017**, *44*, 5550–5560. [CrossRef]

21. Yang, K.; Yao, F.; Wang, J.; Luo, J.; Shen, Z.; Wang, C.; Song, C. Recent dynamics of alpine lakes on the endorheic Changtang Plateau from multi-mission satellite data. *J. Hydrol.* **2017**, *552*, 633–645. [CrossRef]

22. Xiao, Y.; Shao, J.; Frape, S.K.; Cui, Y.; Dang, X.; Wang, S.; Ji, Y. Groundwater origin, flow regime and geochemical evolution in arid endorheic watersheds: A case study from the Qaidam Basin, northwestern China. *Hydrol. Earth Syst. Sci.* **2018**, *22*, 4381–4400. [CrossRef]

23. Zhang, B.; Zhao, D.; Zhou, P.; Qu, S.; Liao, F.; Guangcai, W. Hydrochemical Characteristics of Groundwater and Dominant Water—Rock Interactions in the Delingha. *Water* **2020**, *12*, 836. [CrossRef]

24. Yao, F.; Wang, J.; Yang, K.; Wang, C.; Walter, B.A.; Crétaux, J.F. Lake storage variation on the endorheic Tibetan Plateau and its attribution to climate change since the new millennium. *Environ. Res. Lett.* **2018**, *13*, 064011. [CrossRef]

25. Ma, Y.; Xu, N.; Sun, J.; Wang, X.H.; Yang, F.; Li, S. Estimating water levels and volumes of lakes dated back to the 1980s using Landsat imagery and photon-counting lidar datasets. *Remote Sens. Environ.* **2019**, *232*, 111287. [CrossRef]

26. Xu, N.; Ma, Y.; Zhang, W.; Wang, X.H. Surface-Water-Level Changes during 2003-2019 in Australia Revealed by ICESat/ICESat-2 Altimetry and Landsat Imagery. *IEEE Geosci. Remote Sens. Lett.* **2021**, *18*, 1129–1133. [CrossRef]

27. Paul, F.; Barrand, N.E.; Baumann, S.; Berthier, E.; Bolch, T.; Casey, K.; Frey, H.; Joshi, S.P.; Konovalov, V.; Le Bris, R.; et al. On the accuracy of glacier outlines derived from remote-sensing data. *Ann. Glaciol.* **2013**, *54*, 171–182. [CrossRef]

28. Storey, J.C.; Choate, M.J. Landsat-5 bumper-mode geometric correction. *IEEE Trans. Geosci. Remote Sens.* **2004**, *42*, 2695–2703. [CrossRef]

29. Guan, W.; Cao, B.; Pan, B.; Chen, R.; Shi, M.; Li, K.; Zhao, X.; Sun, X. Updated Surge-Type Glacier Inventory in the West Kunlun Mountains, Tibetan Plateau, and Implications for Glacier Change. *J. Geophys. Res. Earth Surf.* **2022**, *127*, e2021JF006369. [CrossRef]

30. Minora, U.; Bocchiola, D.; D'Agata, C.; Maragno, D.; Mayer, C.; Lambrecht, A.; Vuillermoz, E.; Senese, A.; Compostella, C.; Smiraglia, C.; et al. Glacier Area Stability in the Central Karakoram National Park (Pakistan) in 2001–2010: The "Karakoram Anomaly" in the Spotlight. *Prog. Phys. Geogr.* **2016**, *40*, 629–660. [CrossRef]

31. Du, Y.; Liu, B.; He, W.; Zhou, J.; Duan, S. Analysis on the variation and cause of the lake area in Qaidam Basin from 1976 to 2017. *J. Glaciol. Geocryol.* **2018**, *40*, 1275–1284. [CrossRef]

32. Liu, X.; Wen, Z.; Shu, L.; Lu, C.; Liu, B.; He, H. Analysis of surface area changes of Keluke and Tuosu lakes over past 40 years and influencing factors. *Water Resour. Prot.* **2014**, *30*, 28–33+63.

33. Guo, L.; Wu, Y.; Zheng, H.; Zhang, B.; Wen, M. *An Integrated Dataset of Daily Lake Surface Temperature Over Tibetan Plateau (LSWT_TPv1) (1978~2017)*; National Tibetan Plateau Data Center: Beijing, China, 2021.

34. Haginoya, S.; Fujii, H.; Kuwagata, T.; Xu, J.; Ishigooka, Y.; Kang, S.; Zhang, Y. Air-Lake interaction features found in heat and water exchanges over Nam Co on the Tibetan Plateau. *Sci. Online Lett. Atmos.* **2009**, *5*, 172–175. [CrossRef]

35. Zhu, L.P.; Xie, M.P.; Wu, Y.H. Quantitative analysis of lake area variations and the influence factors from 1971 to 2004 in the Nam Co basin of the Tibetan Plateau. *Chin. Sci. Bull.* **2010**, *55*, 1294–1303. [CrossRef]

36. Monteith, J.L. Evaporation and Environment. The Stage and Movement of Water in Living Organisms. In *Proceedings of the Symposia of the Society for Experimental Biology*; The Company of Biologists: Cambridge, UK, 1965.

37. Penman, H.L. Natural Evaporation from Open Water, Bare Soil and Grass. *Proc. R. Soc. Lond. Ser. A* **1948**, *193*, 120–145.

38. Priestley, C.; Taylor, R.J. On the Assessment of Surface Heat Flux and Evaporation Using Large Scale Parameters. *Mon. Weather. Rev.* **1972**, *100*, 81–92. [CrossRef]

39. De Bruin, H.A.R.; Keijman, J.Q. The Priestley-Taylor Evaporation Model Applied to a Large, Shallow Lake in the Netherlands. *J. Appl. Meteorol. Climatol.* **1979**, *18*, 898–903. [CrossRef]
40. Rosenberry, D.O.; Winter, T.C.; Buso, D.C.; Likens, G.E. Comparison of 15 evaporation methods applied to a small mountain lake in the northeastern USA. *J. Hydrol.* **2007**, *340*, 149–166. [CrossRef]
41. Tian, L.; Yao, T.; MacClune, K.; White, J.W.C.; Schilla, A.; Vaughn, B.; Vachon, R.; Ichiyanagi, K. Stable isotopic variations in west China: A consideration of moisture sources. *J. Geophys. Res. Atmos.* **2007**, *112*, 1–12. [CrossRef]
42. Clarke, I.; Fritz, P. *Environmental Isotope in Hydrogeology*; Springer: Berlin/Heidelberg, Germany, 1997. [CrossRef]
43. Chen, J.; Wang, C.-Y.; Tan, H.; Rao, W.; Liu, X.; Sun, X. New lakes in the Taklamakan Desert. *Geophys. Res. Lett.* **2012**, *39*, 22402. [CrossRef]
44. Chen, J.S.; Wang, C.Y. Rising springs along the Silk Road. *Geology* **2009**, *37*, 243–246. [CrossRef]
45. Zhang, X.; Shi, Y.; Yao, T. Variation of δ 18O in precipitation over the Northeastern Tibetan Plateau. *Sci. China Ser. B* **1995**, *38*, 540–547.
46. Salamon, T. Subglacial conditions and Scandinavian Ice Sheet dynamics at the coarse-grained substratum of the fore-mountain area of southern Poland. *Quat. Sci. Rev.* **2016**, *151*, 72–87. [CrossRef]
47. Post, V.E.A.; Groen, J.; Kooi, H.; Person, M.; Ge, S.; Edmunds, W.M. Offshore fresh groundwater reserves as a global phenomenon. *Nature* **2013**, *504*, 71–78. [CrossRef]
48. Zongyu, C.; Jixiang, Q.; Jianming, X.; Jiaming, X.; Hao, Y.; Yunju, N. Paleoclimatic interpretation of the past 30 ka from isotopic studies of the deep confined aquifer of the North China plain. *Appl. Geochem.* **2003**, *18*, 997–1009. [CrossRef]
49. Currell, M.J.; Cartwright, I.; Bradley, D.C.; Han, D. Recharge history and controls on groundwater quality in the Yuncheng Basin, north China. *J. Hydrol.* **2010**, *385*, 216–229. [CrossRef]
50. Gates, J.B.; Edmunds, W.M.; Darling, W.G.; Ma, J.; Pang, Z.; Young, A.A. Conceptual model of recharge to southeastern Badain Jaran Desert groundwater and lakes from environmental tracers. *Appl. Geochem.* **2008**, *23*, 3519–3534. [CrossRef]
51. Wang, T.; Chen, J.; Zhang, C.; Zhan, L.; Li, L. 14C-Dating Model for Groundwater Affected by CO_2 Inputs From Deep Underground Formations. *Water Resour. Res.* **2020**, *56*, 2–12. [CrossRef]
52. Wang, T.; Chen, J.; Zhang, C. Estimation of fossil groundwater mass fraction accounting for endogenic carbon input across California. *J. Hydrol.* **2021**, *595*, 126034. [CrossRef]
53. Wang, C.; Wang, C.; Manga, M. Coseismic release of water from mountains Evidence from the 1999 (Mw = 7.5) Chi-Chi, Taiwan, earthquake. *Geology* **2004**, *32*, 769–772. [CrossRef]
54. Muir-Wood, R.; King, G. Hydrological signatures of earthquake strain. *J. Geophys. Res. Solid Earth* **1993**, *98*, 22035. [CrossRef]
55. Rojstaczer, S.; Michel, R.; Wolf, S. Permeability enhancement in the shallow crust as a cause of earthquake-induced hydrological changes. *Nature* **1995**, *373*, 237–239. [CrossRef]
56. Manga, M.; Wang, C.-Y. Earthquake hydrology. In *Treatise on Geophysics*; Schubert, G., Ed.; California Institute of Technology: Pasadena, CA, USA, 2007; pp. 293–320.
57. Wang, B.; Ma, Y.; Su, Z.; Wang, Y.; Ma, W. Quantifying the evaporation amounts of 75 high-elevation large dimictic lakes on the Tibetan Plateau. *Sci. Adv.* **2020**, *6*, eaay8558. [CrossRef] [PubMed]
58. Zhao, Z.; Chen, H. Study on Control and Exploration Schemes of Groundwater Level Rising in Gahai Lake Delingha City of Qinghai Province. *Site Investig. Sci. Technol.* **2014**, 45–48.